

13. Tunnels in weak rock

Introduction

Tunnelling in weak rock presents some special challenges to the geotechnical engineer since misjudgements in the design of support systems can lead to very costly failures. To understand the issues involved in the process of designing support for this type of tunnel it is necessary to examine some very basic concepts of how a rock mass surrounding a tunnel deforms and how the support systems act to control this deformation. Once these basic concepts have been explored, examples of practical support designs for different conditions will be considered.

Deformation around an advancing tunnel

Figure 1 shows the results of a three-dimensional finite element analysis of the deformation of the rock mass surrounding a circular tunnel advancing through a weak rock mass subjected to equal stresses in all directions. The plot shows displacement vectors in the rock mass as well as the shape of the deformed tunnel profile. Figure 2 gives a graphical summary of the most important features of this analysis.

Deformation of the rock mass starts about one-half a tunnel diameter ahead of the advancing face and reaches its maximum value about one- and one-half diameters behind the face. At the face position about one-third of the total radial closure of the tunnel has already occurred and the tunnel face deforms inwards as illustrated in Figures 1 and 2. Whether or not these deformations induce stability problems in the tunnel depends upon the ratio of rock mass strength to the in-situ stress level, as will be demonstrated in the following pages.

Note that it is assumed that the deformation process described occurs immediately upon excavation of the face. This is a reasonable approximation for most tunnels in rock. The effects of time dependent deformations upon the performance of the tunnel and the design of the support system will not be discussed in this chapter.

Tunnel deformation analysis

In order to explore the concepts of rock support interaction in a form which can readily be understood, a very simple analytical model will be utilised. This model involves a circular tunnel subjected to a hydrostatic stress field in which the horizontal and vertical stresses are equal.

For the sake of simplicity this analysis is based on the Mohr-Coulomb failure criterion which gives a very simple solution for the progressive failure of the rock mass surrounding the tunnel.

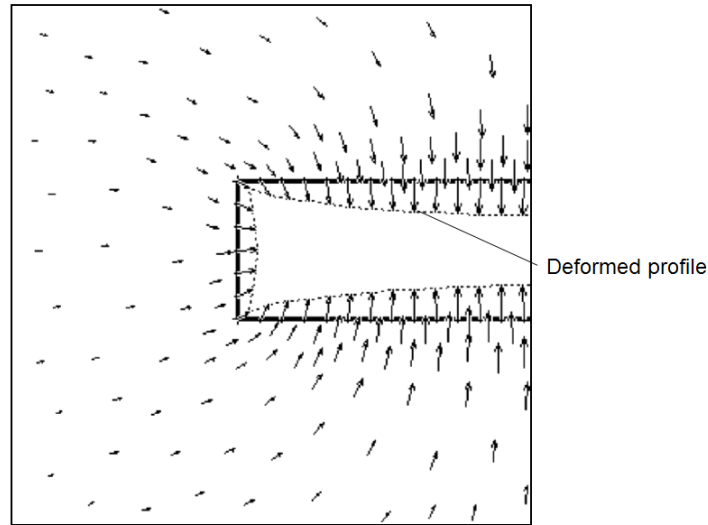


Figure 1: Vertical section through a three-dimensional finite element model of the failure and deformation of the rock mass surrounding the face of an advancing circular tunnel. The plot shows displacement vectors as well as the shape of the deformed tunnel profile.

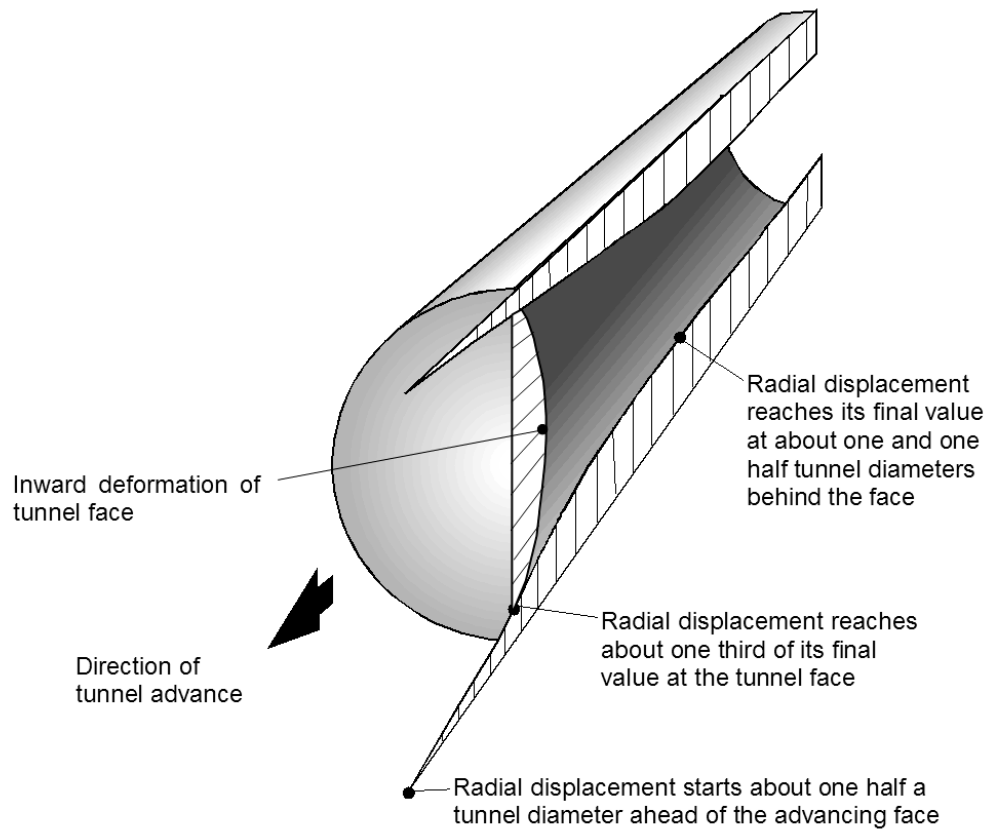


Figure 2: Pattern of deformation in the rock mass surrounding an advancing tunnel.

In this analysis it is assumed that the surrounding heavily jointed rock mass behaves as an elastic-perfectly plastic material in which failure involving slip along intersecting discontinuities is assumed to occur with zero plastic volume change (Duncan Fama, 1993). Support is modelled as an equivalent internal pressure and, although this is an idealised model, it provides useful insights on how support operates.

Definition of failure criterion

It is assumed that the onset of plastic failure, for different values of the effective confining stress σ_3' , is defined by the Mohr-Coulomb criterion and expressed as:

$$\sigma_1' = \sigma_{cm} + k\sigma_3' \quad (1)$$

The uniaxial compressive strength of the rock mass σ_{cm} is defined by:

$$\sigma_{cm} = \frac{2c' \cos \phi'}{(1 - \sin \phi')} \quad (2)$$

and the slope k of the σ_1' versus σ_3' line as:

$$k = \frac{(1 + \sin \phi')}{(1 - \sin \phi')} \quad (3)$$

where σ_1' is the axial stress at which failure occurs

σ_3' is the confining stress

c' is the cohesive strength and

ϕ' is the angle of friction of the rock mass

Analysis of tunnel behaviour

Assume that a circular tunnel of radius r_o is subjected to hydrostatic stresses p_o and a uniform internal support pressure p_i as illustrated in Figure 3. Failure of the rock mass surrounding the tunnel occurs when the internal pressure provided by the tunnel lining is less than a critical support pressure p_{cr} , which is defined by:

$$p_{cr} = \frac{2p_o - \sigma_{cm}}{1 + k} \quad (4)$$

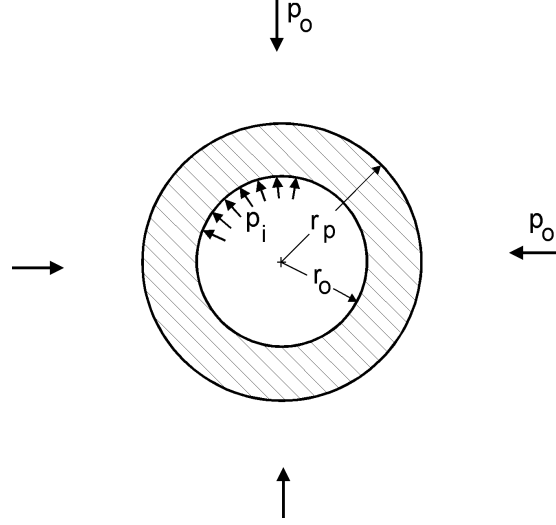


Figure 3: Plastic zone surrounding a circular tunnel.

If the internal support pressure p_i is greater than the critical support pressure p_{cr} , no failure occurs, the behaviour of the rock mass surrounding the tunnel is elastic and the inward radial elastic displacement of the tunnel wall is given by:

$$u_{ie} = \frac{r_o(1+\nu)}{E_m}(p_o - p_i) \quad (5)$$

where E_m is the Young's modulus or deformation modulus and ν is the Poisson's ratio.

When the internal support pressure p_i is less than the critical support pressure p_{cr} , failure occurs and the radius r_p of the plastic zone around the tunnel is given by:

$$r_p = r_o \left[\frac{2(p_o(k-1) + \sigma_{cm})}{(1+k)((k-1)p_i + \sigma_{cm})} \right]^{\frac{1}{(k-1)}} \quad (6)$$

For plastic failure, the total inward radial displacement of the walls of the tunnel is:

$$u_{ip} = \frac{r_o(1+\nu)}{E} \left[2(1-\nu)(p_o - p_{cr}) \left(\frac{r_p}{r_o} \right)^2 - (1-2\nu)(p_o - p_i) \right] \quad (7)$$

A spreadsheet for the determination of the strength and deformation characteristics of the rock mass and the behaviour of the rock mass surrounding the tunnel is given in Figure 4.

Input:	sigci = 10 MPa mu = 0.30 pi = 0.0 MPa	mi = 10 ro = 3.0 m pi/po = 0.00	GSI = 25 po = 2.0 Mpa
Output:	mb = 0.69 k = 2.44 sigcm = 0.69 MPa rp = 6.43 m	s = 0.0000 phi = 24.72 degrees E = 749.9 MPa ui = 0.0306 m	a = 0.525 coh = 0.22 MPa pcr = 0.96 MPa ui= 30.5957 mm
	sigcm/po = 0.3468	rp/ro = 2.14	ui/ro = 0.0102

Calculation:

									Sums
sig3	1E-10	0.36	0.71	1.1	1.43	1.79	2.14	2.50	10.00
sig1	0.00	1.78	2.77	3.61	4.38	5.11	5.80	6.46	29.92
sig3sig1	0.00	0.64	1.98	3.87	6.26	9.12	12.43	16.16	50
sig3sq	0.00	0.13	0.51	1.15	2.04	3.19	4.59	6.25	18

Cell formulae:

```

mb = mi*EXP((GSI-100)/28)
s = IF(GSI>25,EXP((GSI-100)/9),0)
a = IF(GSI>25,0.5,0.65-GSI/200)
sig3 = Start at 1E-10 (to avoid zero errors) and increment in 7 steps of sigci/28 to 0.25*sigci
sig1 = sig3+sigci*(((mb*sig3)/sigci)+s)^a
k = (sumsig3sig1 - (sumsig3*sumsig1)/8)/(sumsig3sq-(sumsig3^2)/8)
phi = ASIN((k-1)/(k+1))*180/PI()
coh = (sigcm*(1-SIN(phi*PI()/180)))/(2*COS(phi*PI()/180))
sigcm = sumsig1/8 - k*sumsig3/8
E = IF(sigci>100,1000*10^((GSI-10)/40),SQRT(sigci/100)*1000*10^((GSI-10)/40))
pcr = (2*po-sigcm)/(k+1)
rp = IF(pi<pcr,ro*(2*(po*(k-1)+sigcm)/((1+k)*((k-1)*pi+sigcm)))^(1/(k-1)),ro)
ui = IF(rp>ro,ro*((1+mu)/E)*(2*(1-mu)*(po-pcr)*((rp/ro)^2)-(1-2*mu)*(po-pi)),ro*(1+mu)*(po-pi)/E)

```

Figure 4: Spreadsheet for the calculation of rock mass characteristics and the behaviour of the rock mass surrounding a circular tunnel in a hydrostatic stress field.

A more elaborate analysis of the same problem, using the Hoek-Brown failure criterion, has been published by Carranza-Torres and Fairhurst (1999) and Carranza-Torres (2004). The details of these analyses are beyond the scope of this discussion, but the results have been incorporated into a program called RocSupport¹ and are used in the following discussion.

Dimensionless plots of tunnel deformation

A useful means of studying general behavioural trends is to create dimensionless plots from the results of parametric studies. One such dimensionless plot is presented in Figure 5. This plot was constructed from the results of a Monte Carlo analysis in which the input parameters for rock mass strength and tunnel deformation were varied at random in 2000 iterations. It is remarkable that, in spite of the very wide range of conditions included in these analyses, the results follow a very similar trend and that it is possible to fit a curve which give a very good indication of the average trend.

¹ Available from www.roscience.com

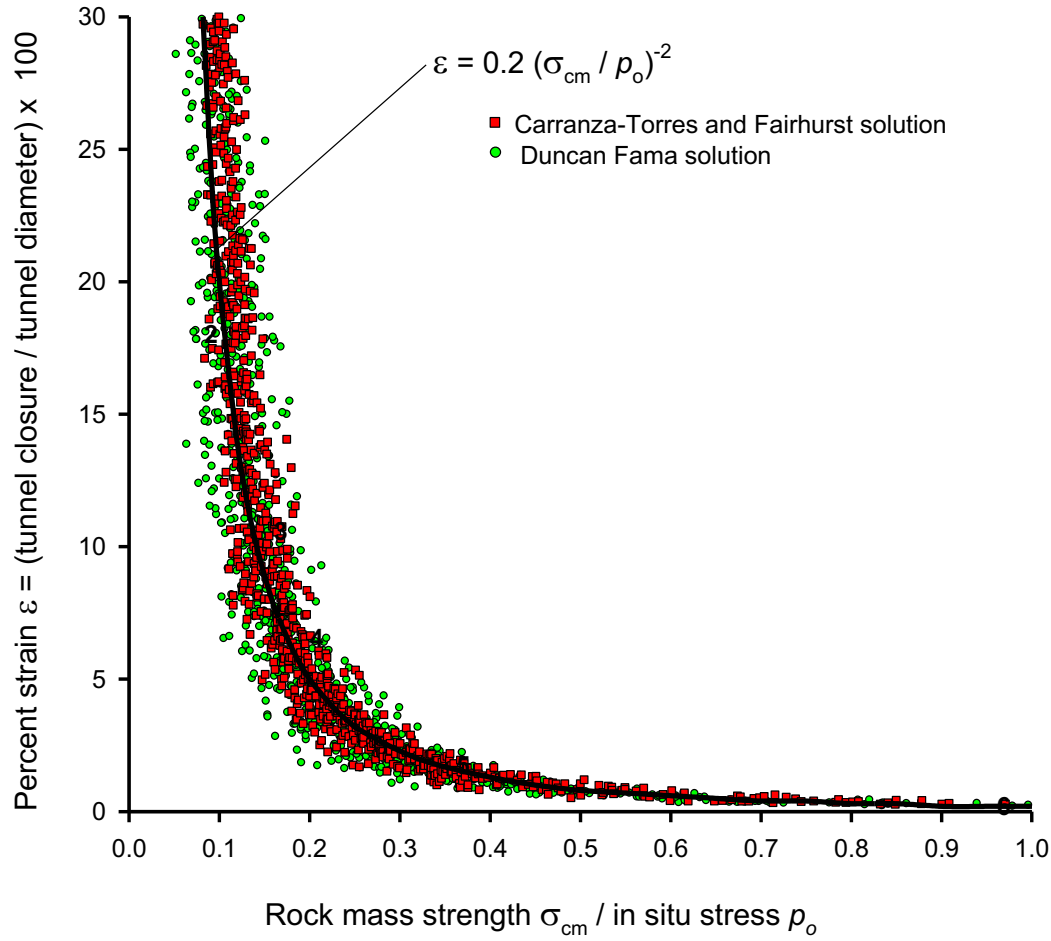


Figure 5: Tunnel deformation versus ratio of rock mass strength to in situ stress based on Monte-Carlo analyses which included a wide range of input parameters².

Figure 5 is a plot of the ratio of tunnel wall displacement to tunnel radius against the ratio of rock mass strength to in-situ stress. Once the rock mass strength falls below 20% of the in-situ stress level, deformations increase substantially and, unless these deformations are controlled, collapse of the tunnel is likely to occur.

Based on field observations and measurements, Sakurai (1983) suggested that tunnel strain levels in excess of approximately 1% are associated with the onset of tunnel instability and with difficulties in providing adequate support. Field observations by Chern et al (1998), plotted in Figure 6, confirm Sakurai's proposal.

² Using the program @RISK in conjunction with a Microsoft Excel spreadsheet for estimating rock mass strength and tunnel behaviour (equations 4 to 7). Uniform distributions were sampled for the following input parameters, the two figures in brackets define the minimum and maximum values used: Intact rock strength σ_{ci} (1,30 MPa), Hoek-Brown constant m_i (5,12), Geological Strength Index GSI (10,35), In situ stress (2, 20 MPa), Tunnel radius (2, 8 m).

Note that some tunnels which suffered strains as high as 5% did not exhibit stability problems. All the tunnels marked as having stability problems were successfully completed but the construction problems increased significantly with increasing strain levels. Hence, the 1% limit proposed by Sakurai is only an indication of increasing difficulty and it should not be assumed that sufficient support should be installed to limit the tunnel strain to 1%. In fact, in some cases, it is desirable to allow the tunnel to undergo strains of as much as 5% before activating the support.

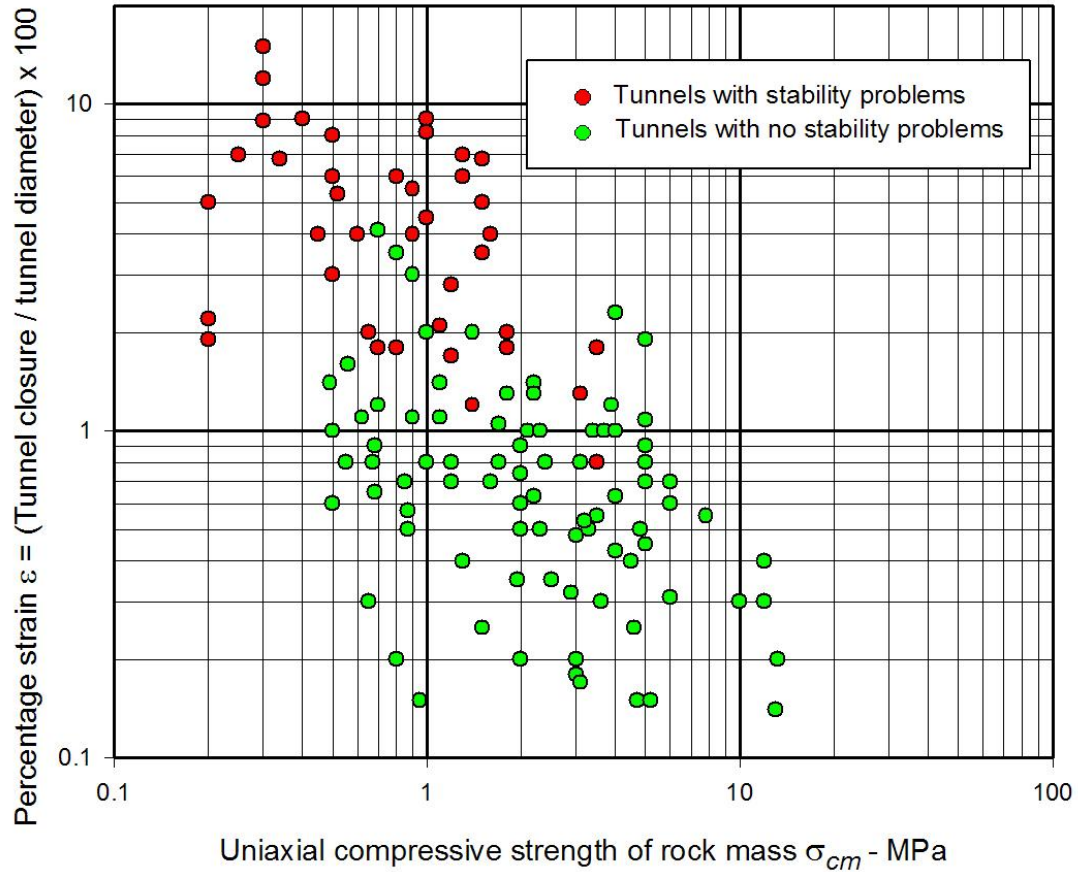


Figure 6: Field observations by Chern et al (1998) from the Second Freeway, Pinglin and New Tienlun headrace tunnels in Taiwan.

Figure 5 is for the condition of zero support pressure ($p_i = 0$). Similar analyses were run for a range of support pressures versus in situ stress ratios (p_i/p_o) and a statistical curve fitting process was used to determine the best fit curves for the generated data for each p_i/p_o value. The resulting curve for tunnel displacement for different support pressures is given in Figure 7.

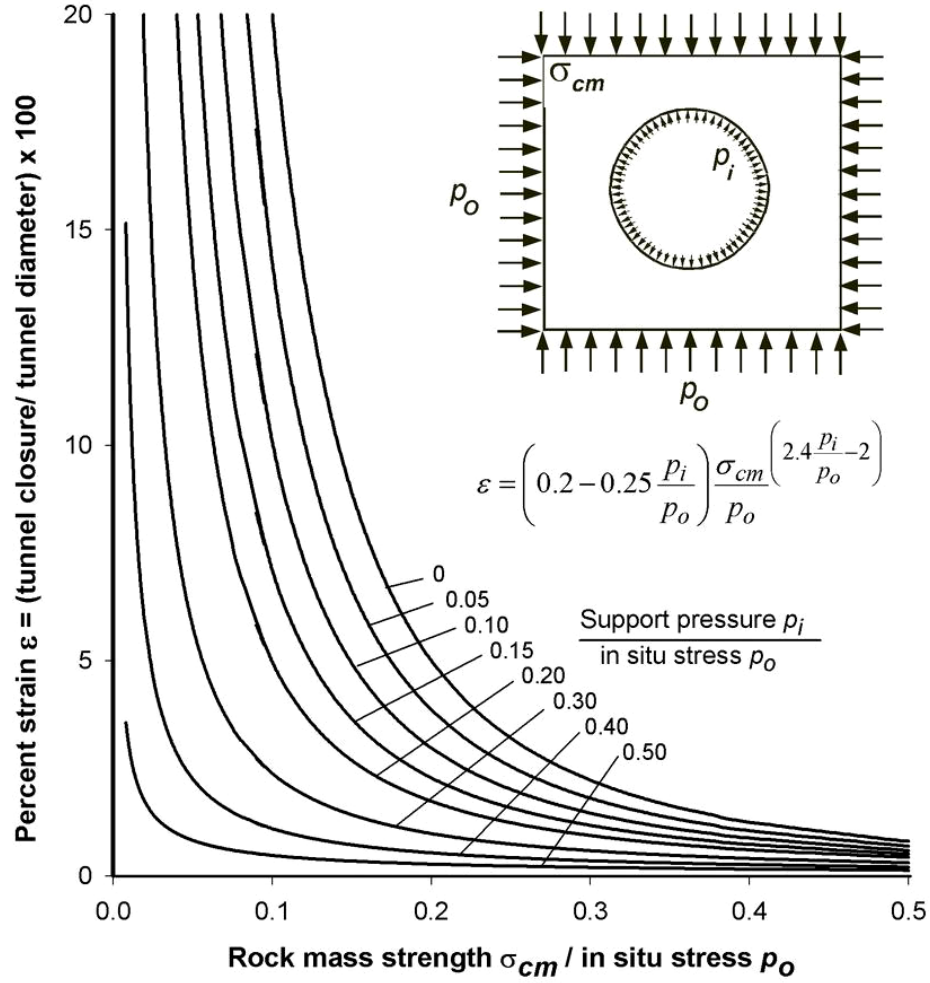


Figure 7: Ratio of tunnel deformation to tunnel radius versus the ratio of rock mass strength to in situ stress for different support pressures.

The series of curves shown in Figures 7 are defined by the equation:

$$\varepsilon\% = \frac{u_i}{r_o} \times 100 = \left(0.2 - 0.25 \frac{p_i}{p_o} \right) \frac{\sigma_{cm}}{p_o} \left(\frac{2.4 \frac{p_i}{p_o} - 2}{p_o} \right) \quad (8)$$

where r_p = Plastic zone radius
 u_i = Tunnel sidewall deformation
 r_o = Original tunnel radius in metres
 p_i = Internal support pressure
 p_o = In situ stress = depth below surface \times unit weight of rock mass
 σ_{cm} = Rock mass strength = $2c' \cos \phi' / (1 - \sin \phi')$

A similar analysis was carried out to determine the size of the plastic zone surrounding the tunnel which is defined by:

$$\frac{rp}{ro} = \left(1.25 - 0.625 \frac{p_i}{p_o} \right) \frac{\sigma_{cm}}{p_o} \left(\frac{p_i}{p_o} \right)^{-0.57} \quad (9)$$

Estimates of support capacity

Hoek and Brown (1980a) and Brady and Brown (1985) have published equations which can be used to calculate the capacity of mechanically anchored rockbolts, shotcrete or concrete linings, or steel sets for a circular tunnel. No useful purpose would be served by reproducing these equations here, but they have been used to estimate the values plotted in Figure 8 (from Hoek, 1998).

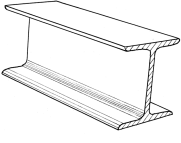
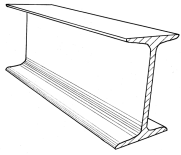
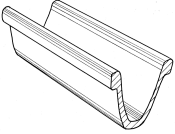
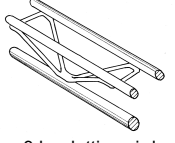
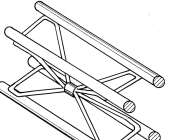
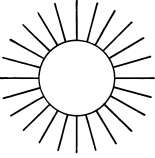
Figure 8 shows maximum support pressures and maximum elastic displacements, p_{sm} and u_{sm} , for different support systems installed in circular tunnels of different diameters. Note that, in all cases, the support is assumed to act over the entire surface of the tunnel walls. In other words, the shotcrete and concrete linings are closed rings, the steel sets are complete circles and the mechanically anchored rockbolts are installed in a regular pattern that completely surrounds the tunnel.


Because this model assumes perfect symmetry under hydrostatic loading of circular tunnels, no bending moments are induced in the support. In reality, there will always be some asymmetric loading, particularly for steel sets and shotcrete placed on rough rock surfaces. Hence, induced bending will result in support capacities that are lower than those given in Figure 8. Furthermore, the effect of not closing the support ring, as is frequently the case, leads to a drastic reduction in the capacity and stiffness of steel sets and concrete or shotcrete linings.

Practical example

In order to illustrate the application of the concepts presented in this chapter, the following practical example is considered.

A 4 m span drainage tunnel is to be driven in the rock mass behind the slope of an open pit mine. The tunnel is at a depth of approximately 150 m below surface and the general rock is a granodiorite of fair quality. A zone of heavily altered porphyry associated with a fault has to be crossed by the tunnel and the properties of this zone, which has been exposed in the open pit, are known to be very poor. Mine management has requested an initial estimate of the behaviour of the tunnel and of the probable support requirements. The following example presents one approach to this problem, using some of the techniques described earlier in this chapter and then expanding them to allow a more realistic analysis of tunnel support behaviour.

Support type	Flange width - mm	Section depth - mm	Weight - kg/m	Curve number	Maximum support pressure $p_{i\max}$ (MPa) for a tunnel of diameter D (metres) and a set spacing of s (metres)
 Wide flange rib	305	305	97	1	$p_{i\max} = 19.9D^{-1.23}/s$
	203	203	67	2	$p_{i\max} = 13.2D^{-1.3}/s$
	150	150	32	3	$p_{i\max} = 7.0D^{-1.4}/s$
 I section rib	203	254	82	4	$p_{i\max} = 17.6D^{-1.29}/s$
	152	203	52	5	$p_{i\max} = 11.1D^{-1.33}/s$
 TH section rib	171	138	38	6	$p_{i\max} = 15.5D^{-1.24}/s$
	124	108	21	7	$p_{i\max} = 8.8D^{-1.27}/s$
 3 bar lattice girder	220	190	19	8	$p_{i\max} = 8.6D^{-1.03}/s$
	140	130	18		
 4 bar lattice girder	220	280	29	9	$p_{i\max} = 18.3D^{-1.02}/s$
	140	200	26		
 Rockbolts or cables spaced on a grid of $s \times s$ metres	34 mm rockbolt			10	$p_{i\max} = 0.354/s^2$
	25 mm rockbolt			11	$p_{i\max} = 0.267/s^2$
	19 mm rockbolt			12	$p_{i\max} = 0.184/s^2$
	17 mm rockbolt			13	$p_{i\max} = 0.10/s^2$
	SS39 Split set			14	$p_{i\max} = 0.05/s^2$
	EXX Swellex			15	$p_{i\max} = 0.11/s^2$
	20mm rebar			16	$p_{i\max} = 0.17/s^2$
	22mm fibreglass			17	$p_{i\max} = 0.26/s^2$
	Plain cable			18	$p_{i\max} = 0.15/s^2$
	Birdcage cable			19	$p_{i\max} = 0.30/s^2$

Support type	Thickness - mm	Age - days	UCS - MPa	Curve number	Maximum support pressure $p_{i\max}$ (MPa) for a tunnel of diameter D (metres)
 Concrete or shotcrete lining	1m	28	35	20	$p_{i\max} = 57.8D^{-0.92}$
	300	28	35	21	$p_{i\max} = 19.1D^{-0.92}$
	150	28	35	22	$p_{i\max} = 10.6D^{-0.97}$
	100	28	35	23	$p_{i\max} = 7.3D^{-0.98}$
	50	28	35	24	$p_{i\max} = 3.8D^{-0.99}$
	50	3	11	25	$p_{i\max} = 1.1D^{-0.97}$
	50	0.5	6	26	$p_{i\max} = 0.6D^{-1.0}$

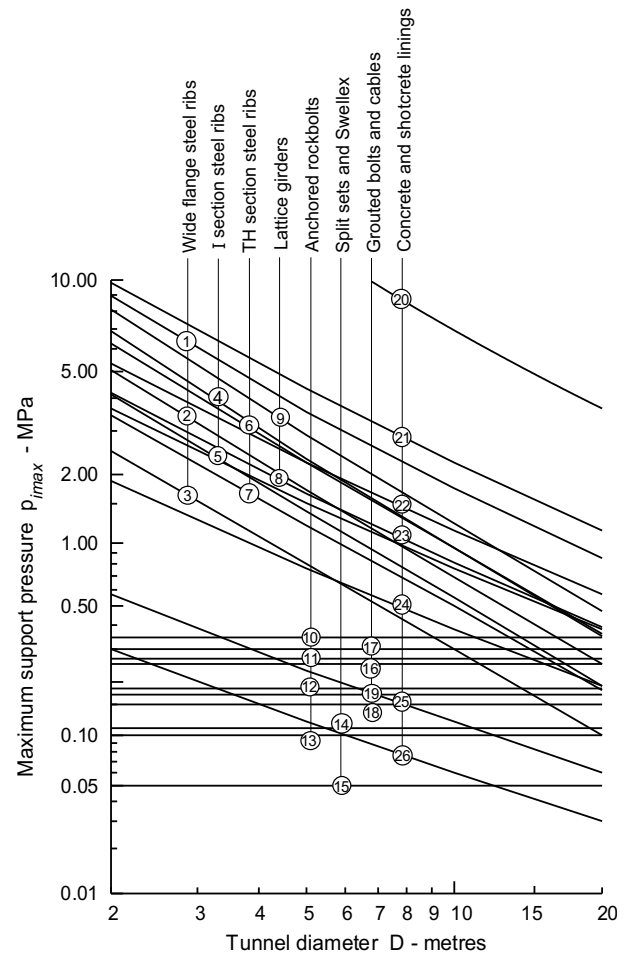


Figure 8: Approximate maximum capacities for different support systems installed in circular tunnels. Note that steel sets and rockbolts are all spaced at 1 m.

Estimate of rock mass properties

Figures 5 and 7 show that a crude estimate of the behaviour of the tunnel can be made if the ratio of rock mass strength to in situ stress is available. For the purpose of this analysis, the in-situ stress is estimated from the depth below surface and the unit weight of the rock. For a depth of 150 m and a unit weight of 0.027 MN/m^3 , the vertical in situ stress is approximately 4 MPa. The fault material is considered incapable of sustaining high differential stress levels and it is assumed that the horizontal and vertical stresses are equal within the fault zone.

In the case of the granodiorite, the laboratory uniaxial compressive strength is approximately 100 MPa. However, for the fault material, specimens can easily be broken by hand as shown in Figure 9. The laboratory uniaxial compressive strength of this material is estimated at approximately 10 MPa.

Based upon observations in the open pit mine slopes and utilizing the procedures described in the chapter on 'Rock mass properties', the granodiorite is estimated to have a GSI value of approximately 55. The fault zone, shown in Figure 9, has been assigned GSI = 15.



Figure 9: Heavily altered porphyry can easily be broken by hand.

The program RocLab³ implements the methodology described in the chapter on ‘Rock mass properties’ and, in particular, the equations given in the 2002 version of the Hoek-Brown failure criterion (Hoek et al, 2002). This program has been used to calculate the global rock mass strength σ_{cm} for the granodiorite and the fault zone. The results are presented below:

Material	σ_{ci} - MPa	GSI	m_i	σ_{cm}	σ_{cm}/p_0
Granodiorite	100	55	30	33	8.25
Fault	10	15	8	0.6	0.15

Support requirements

Figures 5 and 6 show that, for the granodiorite with a ratio of rock mass strength to in situ stress of 8.25, the size of the plastic zone and the induced deformations will be negligible. This conclusion is confirmed by the appearance of an old drainage tunnel that has stood for several decades without any form of support. Based upon this evaluation, it was decided that no permanent support was required for the tunnel in the fair quality granodiorite. Spot bolts and shotcrete were installed for safety where the rock mass was more heavily jointed. The final appearance of the tunnel in granodiorite is shown in Figure 10.



Figure 10: Appearance of the drainage tunnel in fair quality granodiorite in which no permanent support was required. Spot bolts and shotcrete were installed for safety in jointed areas. The concrete lined drainage channel is shown in the centre of the tunnel floor.

³ This program can be downloaded from www.rocscience.com.

In the case of the altered porphyry and fault material, the ratio of rock mass strength to in situ stress is 0.15. From Equation 9 the radius of plastic zone for a 2 m radius tunnel in this material is approximately 7.4 m without support. The tunnel wall deformation is approximately 0.18 m which translates into a tunnel strain of $(0.18/2) * 100 = 9\%$.

Based on the observations by Sakurai (1983) and Chern et al (1998), the predicted strain of 9% for the mine drainage tunnel discussed earlier is clearly unacceptable and substantial support is required in order to prevent convergence and possible collapse of this section. Since this is a drainage tunnel, the final size is not a major issue and a significant amount of closure can be tolerated.

An approach that is frequently attempted, in such cases, is to install sufficient support behind the face of the tunnel to limit the strain to an acceptable level. Assuming a practical limit of 2% strain (from Figure 6), equation 8 and Figure 7 show that, for $\sigma_{cm}/p_o = 0.15$, an internal support pressure of approximately $p_i/p_o = 0.25$ is required to support the tunnel. For $p_o = 4$ MPa this means a support pressure $p_i = 1$ MPa.

Figure 8 shows that, for a 4 m diameter tunnel, a support in excess of 1 MPa can only be provided by a passive system of steel, sets, lattice girders, shotcrete or concrete lining or by some combination of these systems. These systems have to be installed in a fully closed ring (generally in a circular tunnel) in order to act as a load bearing structure. Rockbolts or cables, even assuming that they could be anchored in the fault material, cannot provide this level of equivalent support.

There are several problems associated with the installation of heavy passive support in this particular tunnel. These are:

1. The remainder of the drainage tunnel is horseshoe shaped as shown in Figure 10. Changing the section to circular for a relative short section of fault zone is not a very attractive proposition because of the limitations this would impose on transportation of equipment and materials through the zone.
2. The use of heavy steel sets creates practical problems in terms of bending the sets into the appropriate shape. A practical rule of thumb is that an H or I section can only be bent to a radius of approximately 14 times the depth of the section. Figure 11 which shows a heavy H section set being bent and there is significant buckling of the inside flange of the set.
3. The use of shotcrete or concrete lining is limited by the fact that it takes time for these materials to harden and to achieve the required strength required to provide adequate support. The use of accelerators or of thick linings can partially overcome these problems, but may introduce another set of practical problems.

The practical solution adopted in the actual case upon which this example is based was to use sliding joint top hat section sets. These sets, as delivered to site, are shown in Figure 12 which illustrates how the sections fit into each other. The assembly of these sets to form a sliding joint is illustrated in Figure 14 and the installation of the sets in the tunnel is illustrated in Figure 15.



Figure 12: Buckling of an H section steel set being bent to a small radius. Temporary stiffeners have been tack welded into the section to minimise buckling but a considerable amount of work is required to straighten the flanges after these stiffeners have been removed.

Figure 13 Top hat section steel sets delivered to site ready to be transported underground.



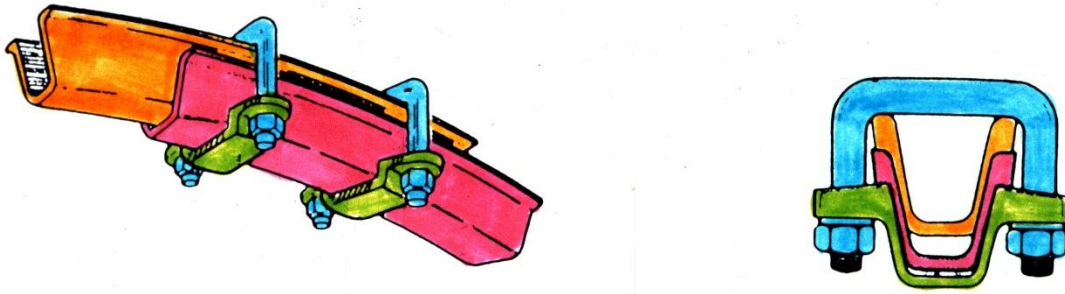


Figure 14 Assembly of a sliding joint in a top hat section steel set.



Figure 15: Installation of sliding joint top hat section steel sets immediately behind the face of a tunnel being advanced through very poor quality rock.

The sets are installed immediately behind the advancing face which, in a rock mass such as that considered here, is usually excavated by hand. The clamps holding the joints are tightened to control the frictional force in the joints which slide progressively as the face is advanced and the rock load is applied to the sets.

The use of sliding joints in steel sets allows very much lighter section sets to be used than would be the case for sets with rigid joints. These sets provide immediate protection for the workers behind the face, but they permit significant deformation of the tunnel to take place as the face is advanced. In most cases, a positive stop is welded onto the sets so that, after a pre-determined amount of deformation has occurred, the joint locks and the set becomes rigid. A trial-and-error process has to be used to find the amount of deformation that can be permitted before the set locks. Too little deformation will result in obvious buckling of the set while too much deformation will result in loosening of the surrounding rock mass.

In the case of the tunnel illustrated in Figure 15, lagging behind the sets consists of wooden poles of approximately 100 mm diameter. A variety of materials can be used for lagging but wood, in the form of planks or poles, is still the most common material used in mining. In addition to the lagging, a timber mat has been propped against the face to improve the stability of the face. This is an important practical precaution since instability of the tunnel face can result in progressive ravelling ahead of the steel sets and, in some cases, collapse of the tunnel.

The way in which sliding joints work is illustrated diagrammatically in Figure 16.

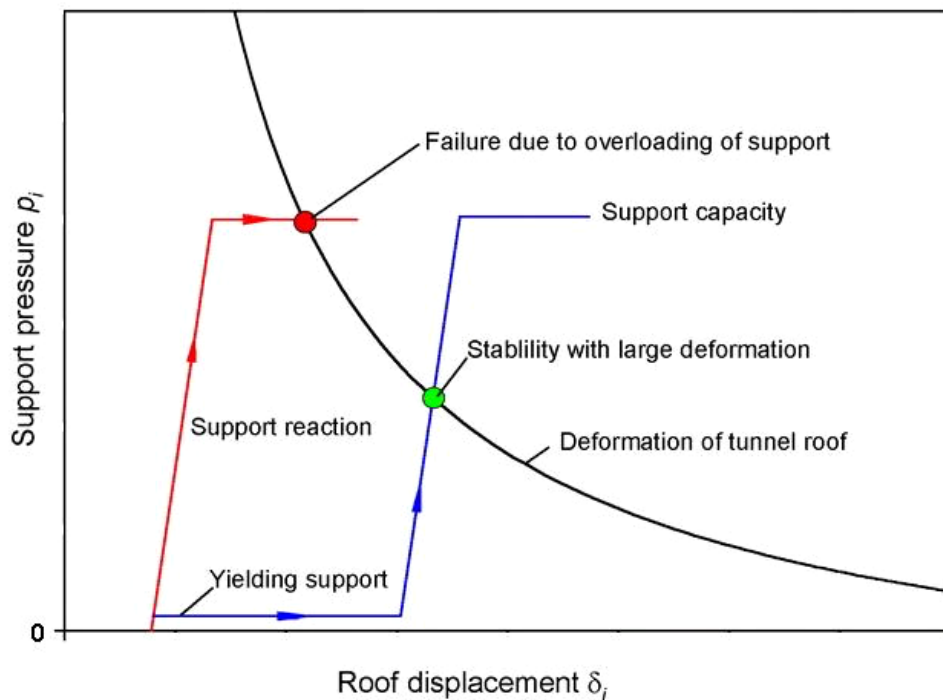


Figure 16: Delay in the activation of passive support by the use of sliding joints.

Figure 16 shows that passive support in the form of steel sets, lattice girders, shotcrete or concrete linings can fail if installed too close to the face (red lines). This is because the support pressure required to achieve stability is larger than the capacity of the support system. As the displacements in the tunnel increase as the face moves away from the section under consideration, the support pressure required to achieve equilibrium decreases as illustrated by the curve in Figure 16. Delaying the activation of the support system, using sliding joints (blue line), can stabilize the tunnel at support pressures within the capacity of the support.

Many systems have been used to introduce these yielding elements into tunnels with squeezing problems. An example is the use of sliding joints in steel sets as shown in Figure 16. Another system is to use “stress controllers” in which controlled buckling of an inner steel tube provides the yielding required and the system locks and becomes more rigid when a pre-determined deformation has occurred. This system, developed by Professor Wulf Schubert (Schubert, 1996) at the University of Graz in Austria, is illustrated in Figures 17 and 18.



Figure 17: A row of stress controllers installed in a slot in the shotcrete lining in a tunnel



Figure 18: Section through a stress controller showing the buckling inner tube. After Schubert, 1996.

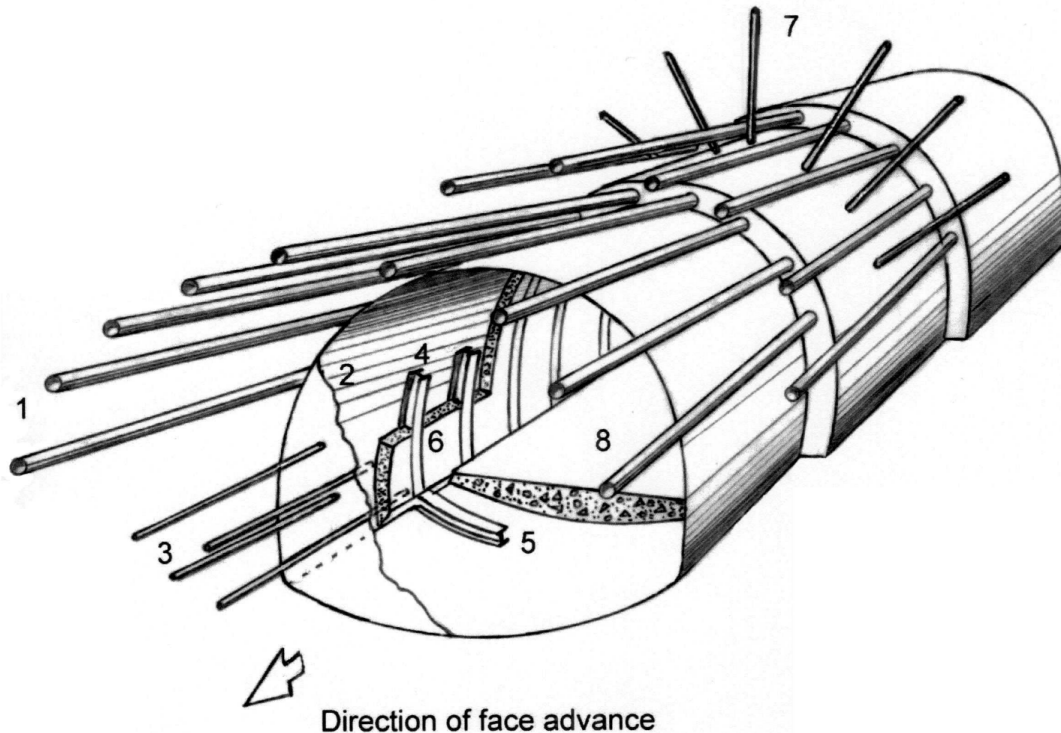
As an alternative to supporting the face, as illustrated in Figure 15, spiles or forepoles can be used to create an umbrella of reinforced rock ahead of the advancing face. Figure 19 illustrate the general principles of the technique. In the example illustrated, spiling is being used to advance a 7 m span, 3 m high tunnel top heading through a clay-rich fault zone material in a tunnel in India. The spiles, consisting of 25 mm steel bars, were driven in by means of a heavy sledgehammer.



Figure 19: Spiling in very poor quality clay-rich fault zone material.

Figure 20 shows a more elaborate system used in large span tunnels in poor quality rock masses. This system relies on grouted fiberglass dowels, which can be cut relatively easily, to stabilize the face ahead of the tunnel and grouted forepoles to provide a protective umbrella over the face. These forepoles consist of 75 to 140 mm diameter steel pipes through which grout is injected. In order for the forepoles to work effectively the rock mass should behave in a frictional manner so that arches or bridges can form between individual forepoles. The technique is not very effective in fault gouge material containing a significant proportion of clay unless the forepole spacing is very close. The forepoles are installed by means of a special drilling machine as illustrated in Figure 21.

While these forepole umbrella systems can add significantly to the cost of driving tunnels and can also result in very slow advance rates, they have been used very successfully in driving many transportation tunnels in Europe (Carrieri et al, 1991).



- 1 Forepoles – typically 75- or 114-mm diameter pipes, 12 m long installed every 8 m along the tunnel to create a 4 m overlap between successive forepole umbrellas.
- 2 Shotcrete – applied immediately behind the face and to the face, in cases where face stability is a problem. Typically, this initial shotcrete layer is 25 to 50 mm thick.
- 3 Grouted fiberglass dowels – Installed midway between forepole umbrella installation steps to reinforce the rock immediately ahead of the face. These dowels are usually 6 to 12 m long and are spaced on a 1 m x 1 m grid.
- 4 Steel sets – installed as close to the face as possible and designed to support the forepole umbrella and the stresses acting on the tunnel.
- 5 Invert struts – installed to control floor heave and to provide a footing for the steel sets.
- 6 Shotcrete – typically steel fibre reinforced shotcrete applied as soon as possible to embed the steel sets to improve their lateral stability and also to create a structural lining.
- 7 Rockbolts as required. In very poor-quality rock, it may be necessary to use self-drilling rockbolts in which a disposable bit is used and is grouted into place with the bolt.
- 8 Invert lining – either shotcrete or concrete can be used, depending upon the end use of the tunnel.

Figure 20: Full face 10 m span tunnel excavation through weak rock under the protection of a forepole umbrella. The final concrete lining is not included in this figure.



Figure 21: Installation of 12 m long 75 mm diameter pipe forepoles in an 11 m span tunnel top heading in a fault zone.

References

- Brady, B.H.G. and Brown, E.T. 1985. *Rock mechanics for underground mining*. London: Allen and Unwin.
- Carranza-Torres, C. and Fairhurst, C. 1999. The elasto-plastic response of underground excavations in rock masses that satisfy the Hoek-Brown failure criterion. *Int. J. Rock Mech. Min. Sci.* **36**(6), 777–809.
- Carranza-Torres, C. 2004. Elasto-plastic solution of tunnel problems using the generalized form of the Hoek-Brown failure criterion. In proc. ISRM SINOROCK2004 symposium China, (Eds. J.A. Hudson and F. Xia-Ting). *Int. J. Rock Mech. Min. Sci.* **41**(3), 480–481.
- Carranza-Torres, C. 2004. Some Comments on the Application of the Hoek-Brown Failure Criterion for Intact Rock and Rock Masses to the Solution of Tunnel and Slope Problems. In *MIR 2004 – X conference on rock and engineering mechanics*, Torino, (eds. G. Barla and M. Barla). Chapter 10, 285–326. Pàtron Editore. Bologna: Pàtron Editore.

- Chern, J.C., Yu, C.W., and Shiao, F.Y. 1998. Tunnelling in squeezing ground and support estimation. *Proc. reg. symp. sedimentary rock engineering*, Taipei, 192-202.
- Duncan Fama, M.E. 1993. Numerical modelling of yield zones in weak rocks. In *Comprehensive rock engineering*, (ed. J.A. Hudson) **2**, 49-75. Oxford: Pergamon.
- Hoek, E. and Brown, E.T. 1980. *Underground excavations in rock*. London: Instn Min. Metall.
- Hoek, E. and Brown, E.T. 1997. Practical estimates of rock mass strength. *Int. J. Rock Mech. & Mining Sci. & Geomech. Abstr.* **34**(8), 1165-1186.
- Hoek, E. 1998. Tunnel support in weak rock, keynote address, *Symp. On sedimentary rock engineering*. Taipei, Taiwan, 20-22.
- Hoek, E., Carranza-Torres, C.T., Corkum, B. Hoek-Brown failure criterion-2002 edition. In *Proceedings of the Fifth North American Rock Mechanics Symp.*, Toronto, Canada, **1**: 267-73.
- Carrieri, G., Grasso, P., Mahtab, A. and Pelizza, S. 1991. Ten years of experience in the use of umbrella-arch for tunnelling. *Proc. SIG Conf. On Soil and Rock Improvement*, Milano **1**, 99-111.
- Sakurai, S. 1983. Displacement measurements associated with the design of underground openings. *Proc. Int. Symp. Field Measurements in Geomechanics*, Zurich, **2**, 1163-1178.
- Schubert, W. 1996. Dealing with squeezing conditions in Alpine tunnels. *Rock Mech. Rock Engng.* **29**(3), 145-153.